

# Alfvén modes and wave particle interaction in a tokamak

**Meng Li**

**Advisor:** *Boris N. Breizman*

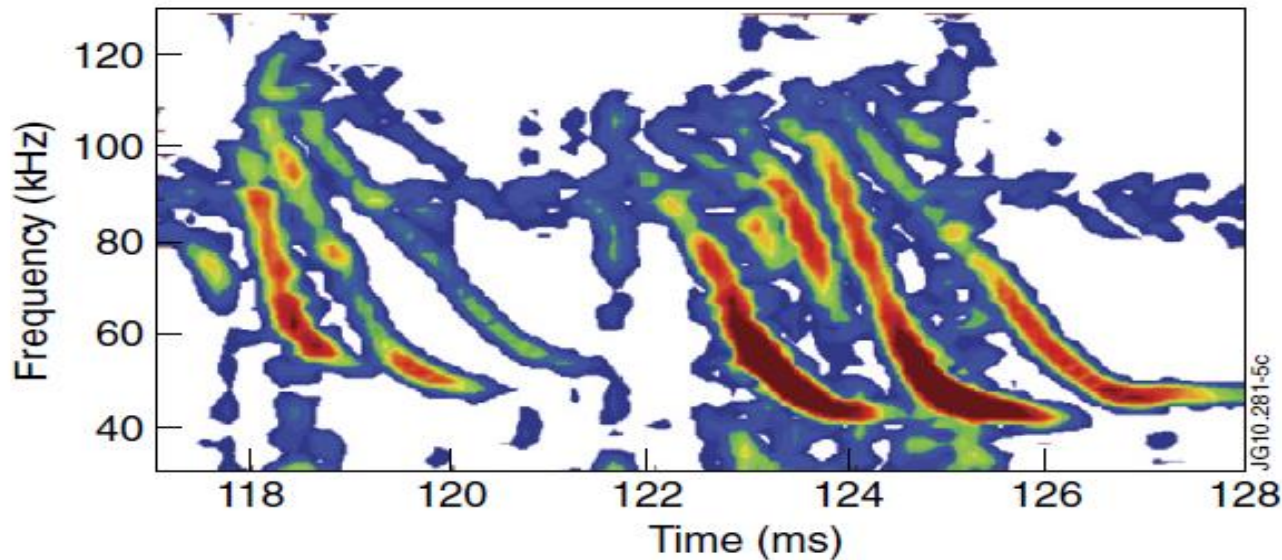
*Institute for Fusion Studies, The University of  
Texas at Austin*



# Background

- Energetic particles can be produced by fusion reaction(3.5 MeV alpha particles) or auxiliary heating process (ICRH or NBI).
- Fast particles can resonate with Alfvénic modes and excite instabilities that may result in significant energetic particle transport.
- The existence of Toroidal Alfvén Eigenmodes(TAEs) driven by fast ions in burning plasmas has been convincingly confirmed in experiment.
- Due to nonlinear wave-particle interaction, the wave frequency can have considerable sweeping.

# Motivation



NBI-driven modes with downward frequency sweeping on MAST

**We need to describe the resonant response of energetic particles, and integrated with MHD equations for self-consistent simulation of the nonlinear wave particle interaction.**

# Outline

- **MHD stability analysis for Alfvénic Modes**
  1. AEGIS framework
  2. Continuum absorption near TAE gap
- **Energetic Particle dynamics**
  1. Canonical Straight field line coordinates
  2. Scheme for constructing Action-Angle variables

# Outline

- **MHD stability analysis for Alfvénic Modes**
  1. AEGIS framework
  2. Continuum absorption near TAE gap
- **Energetic Particle dynamics**
  1. Canonical Straight field line coordinates
  2. Scheme for constructing Action-Angle variables

# Introduction to AEGIS

- **AEGIS\*** is an ideal MHD eigenvalue code with an adaptive grid mesh in radial direction, and Fourier decomposition in the poloidal and toroidal directions.
- It uses the shooting method radially to get the independent solution in different regions and construct an appropriate linear combination of the solutions.
- AEGIS code is used for linear MHD stability analysis, for example, Alfvénic cascades in MST. And we found that pressure gradient has opposite effects on the  $n = 4$  and  $n = 5$  modes observed in experiment.

\*L.J. Zheng and M. Kotschenreuther, *J. Comp. Phys.* 211 (2006) 748

# Outline

- **MHD stability analysis for Alfvénic Modes**
  1. AEGIS framework
  2. Continuum absorption near TAE gap
- **Energetic Particle dynamics**
  1. Canonical Straight field line coordinates
  2. Scheme for constructing Action-Angle variables

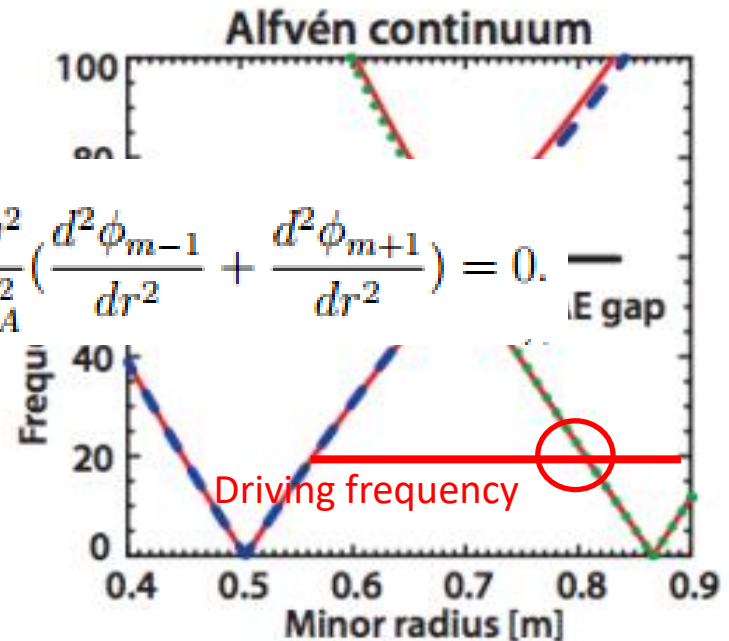
# Shear Alfvén continuum

- Local dispersion relation for shear Alfvén wave:

$$\omega_A = k_{\parallel} v_A$$

$$\frac{d}{dr} \left[ \left( \frac{\omega^2}{v_A^2} - k_{\parallel m}^2 \right) \frac{d\phi_m}{dr} \right] - \frac{m^2}{r^2} \left( \frac{\omega^2}{v_A^2} - k_{\parallel m}^2 \right) \phi_m + \hat{\epsilon} \frac{\omega^2}{v_A^2} \left( \frac{d^2 \phi_{m-1}}{dr^2} + \frac{d^2 \phi_{m+1}}{dr^2} \right) = 0.$$

- Toroidicity couples neighboring poloidal branches and forms a gap in the spectrum where toroidicity-induced Alfvén eigenmodes (TAE) reside.



- Continuum Absorption/Damping:** For a periodic perturbation at frequency  $\omega$ , energy is resonantly absorbed at the continuum crossing where  $\omega = \omega_A$ .

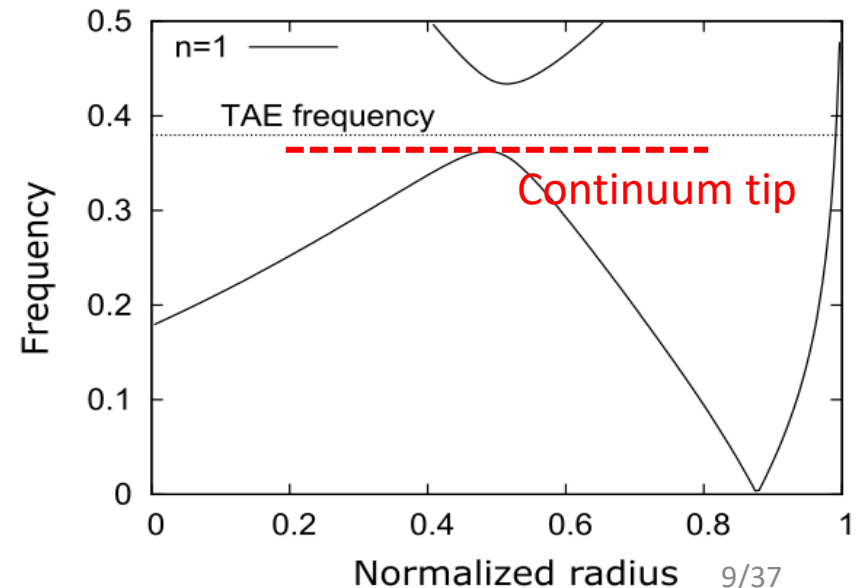


# Continuum absorption near TAE gap

- For energetic particle mode in the continuum, proper evaluation of continuum absorption is required.
- Furthermore, when the frequency matches the tip-like structure in the TAE gap, how much is the continuum absorption then?

- **Challenge:**

- ❖ numerically calculate the continuum absorption with AEGIS, even when frequency goes to the tip of the continuum spectrum.



# Modification of AEGIS framework

- I add an oscillating external source current with frequency  $\omega$ , the MHD equation for plasma displacement  $\xi$  becomes:

$$\mu_0 \rho \frac{d^2 \xi}{dt^2} = \underbrace{[\nabla \times \nabla \times (\xi \times B)] \times B + (\nabla \times B) \times [\nabla \times (\xi \times B)]}_{\text{MHD force operator } \hat{L}\xi} - \underbrace{(\delta \mathbf{J}_\omega e^{-i\omega t} + \text{c.c.}) \times B}_{\text{Source term } \delta \mathbf{J}}.$$

- I introduce a small friction force  $-\rho\gamma\mathbf{v}$  by adding a positive imaginary part  $\Upsilon$  in frequency, with  $\Upsilon \ll \omega$ .

$$\rho \frac{d\mathbf{v}}{dt} + \rho\gamma\mathbf{v} = \hat{L}\xi + \delta \mathbf{J}.$$

- The adaptive grids in AEGIS enables us to get accurate result with relatively small  $\Upsilon \sim 10^{-5} \omega$ .
- The dissipative power of the friction force:

$$Q = \int \rho\gamma\mathbf{v} \cdot \mathbf{v} dV = \int \frac{1}{2} \rho\gamma\omega^2 \xi_\omega^* \cdot \xi_\omega dV.$$

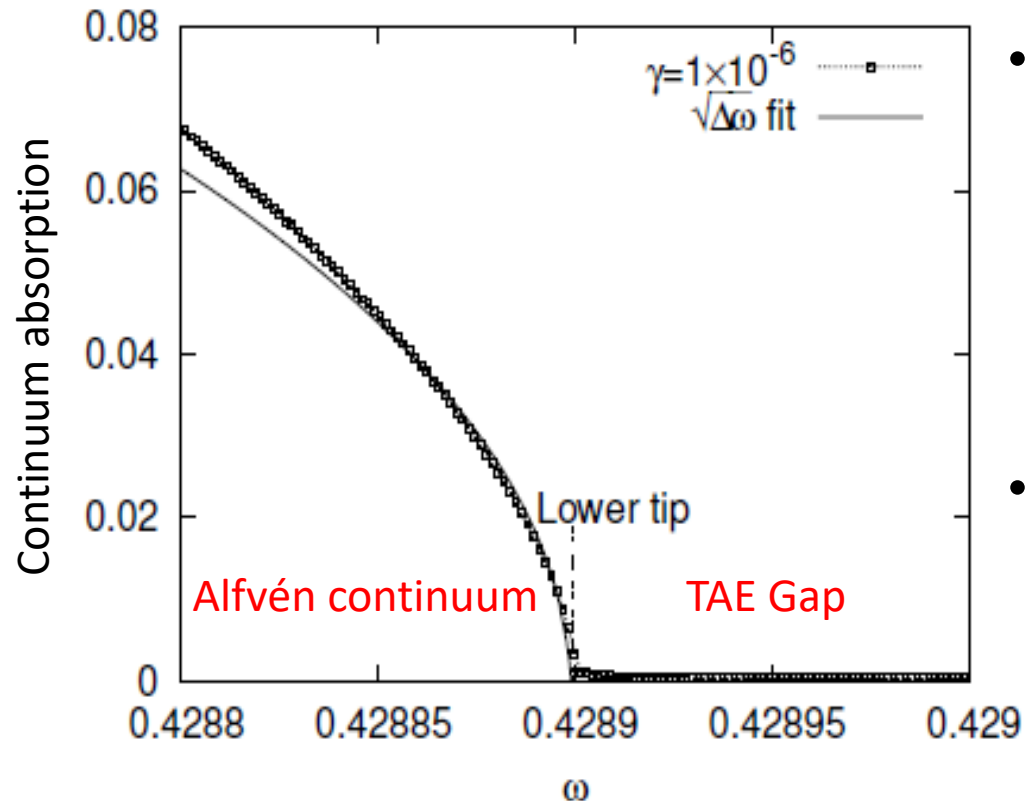
represents the continuum absorption in the limit of  $\Upsilon \rightarrow 0$

# Theoretical consideration of tip absorption

- With analytical simplification, continuum absorption is inversely proportional to the slope of Alfvén continuum at the crossing point( $d\omega_A/dr$ ) away from the gap.
- **Continuum tip absorption generally does not go to infinity though the slope of the continuum is zero at the tip, and the lower and upper tips of the TAE gap can have very different continuum absorption features.\***
- The difference result from an eigenmode whose frequency can be arbitrarily close to the upper tip whereas the lower tip is always a finite distance away from the closest eigenmode.

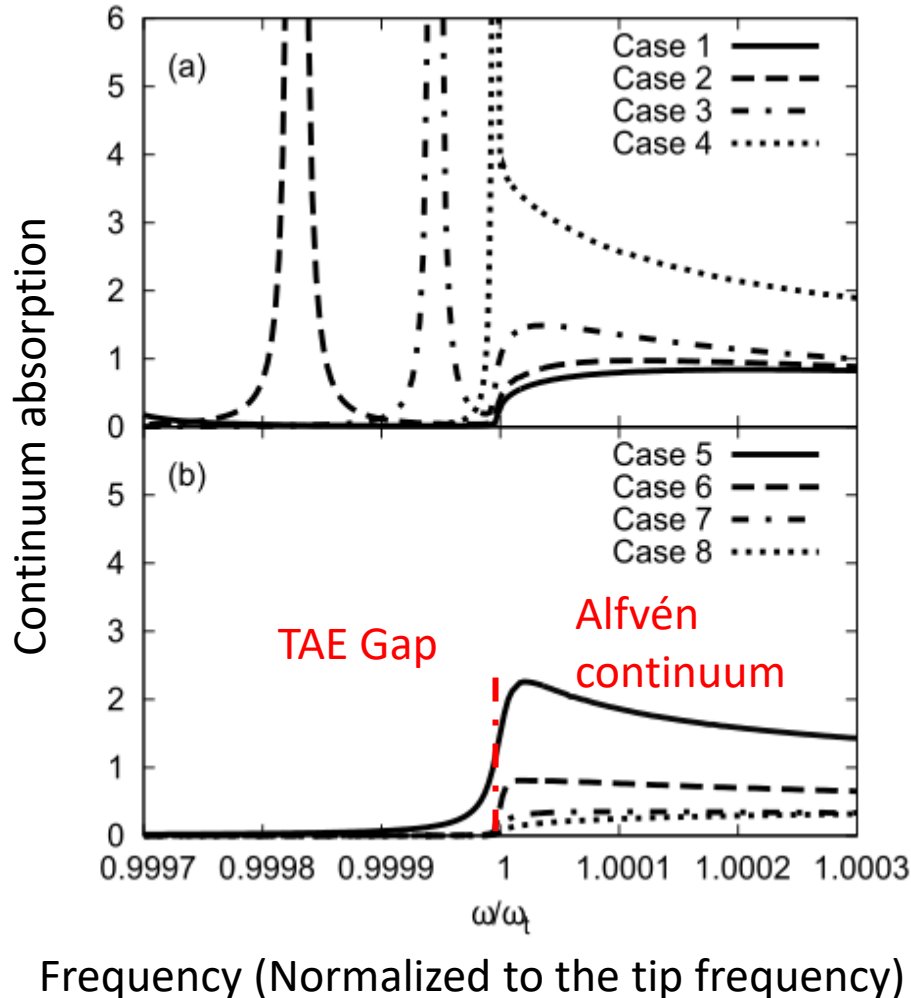
\*M. Li, B. N. Breizman, L. J. Zheng, *et al.* , *New J. Phys.* 103596.R1 (2015)

# Lower tip absorption from AEGIS



- Lower tip absorption has nice  $\sqrt{\Delta\omega}$  scaling below the lower tip and vanishes at the tip.
- We find the lower tip absorption pattern doesn't change significantly as parameters change.

# Upper tip absorption from AEGIS



- We vary the equilibrium profile (from Case 1 to Case 8) to change the upper TAE frequency.
- **The absorption pattern changes dramatically as the upper TAE frequency moves upward and merges into the continuum.**
- **The results indicate that AEGIS can handle continuum absorption problem for Alfvénic waves pretty well.**

# Outline

- **MHD stability analysis for Alfvénic Modes**
  1. AEGIS framework
  2. Continuum absorption near TAE gap
- **Energetic Particle dynamics**
  1. Canonical Straight field line coordinates
  2. Scheme for constructing Action-Angle variables

# Guiding center Lagrangian

Recall the gyro-averaged Littlejohn Lagrangian for the particle guiding center motion:

$$L = \frac{e}{c} \mathbf{A} \cdot \dot{\mathbf{X}} + mv_{\parallel} \mathbf{b} \cdot \dot{\mathbf{X}} + \frac{mc}{e} \mu \dot{\xi} - \mu B - \frac{1}{2} mv_{\parallel}^2 - e\phi. \quad (1)$$

with the dynamical variables:

- $\mathbf{X}$  is the guiding center position
- $v_{\parallel}$  is the parallel velocity along the magnetic field.
- $\xi$  is the gyroangle.
- $\mu$  is the magnetic moment.
- $\mathbf{b} = \mathbf{B}/B$  is the direction of the magnetic field,  $\mathbf{A}$  is vector potential,  $\phi$  is the scalar potential.

# Hamiltonian form for GC motion

- There are six dynamical variables for the guiding center motion.
- The six dynamical variables do not immediately split into three canonical pairs for Hamiltonian formalism, because **the Littlejohn Lagrangian generally contains four time derivatives rather than three.**
- The general step to achieve Hamiltonian form is to eliminate  $\dot{\psi}$  in the Lagrangian.



# White & Boozer approach

- Roscoe White and Allen Boozer proposed that in Boozer coordinates

$$\mathbf{A} = A_\theta \nabla \theta + A_\zeta \nabla \zeta; \quad \mathbf{B} = \delta \nabla \psi + B_\theta \nabla \theta + B_\zeta \nabla \zeta,$$

$\delta$  doesn't affect the guiding center trajectory and can be neglected, so that  $\dot{\psi} = \nabla \psi \cdot \dot{\mathbf{X}}$  term doesn't appear in the Littlejohn Lagrangian.

- Then the Littlejohn Lagrangian in equilibrium field can be approximate by

$$L = P_\theta \dot{\theta} + P_\zeta \dot{\zeta} + \frac{mc}{e} \mu \dot{\xi} - H(P_\zeta, P_\theta, \theta, \mu)$$

and then derive the guiding center equation of motion.\*

- However, simply dropping  $\delta$  will result in the modification of the frequency of guiding center motion.**

# Canonical field coordinates approach

- A rigorous way is to find canonical field coordinates in which the **covariant components of the radial magnetic field  $B_\psi$  vanishes**, so that:

$$\mathbf{A} = A_\theta \nabla \theta + A_\zeta \nabla \zeta$$

$$\mathbf{B} = B_\theta \nabla \theta + B_\zeta \nabla \zeta$$

Then, for the unperturbed guiding center motion:

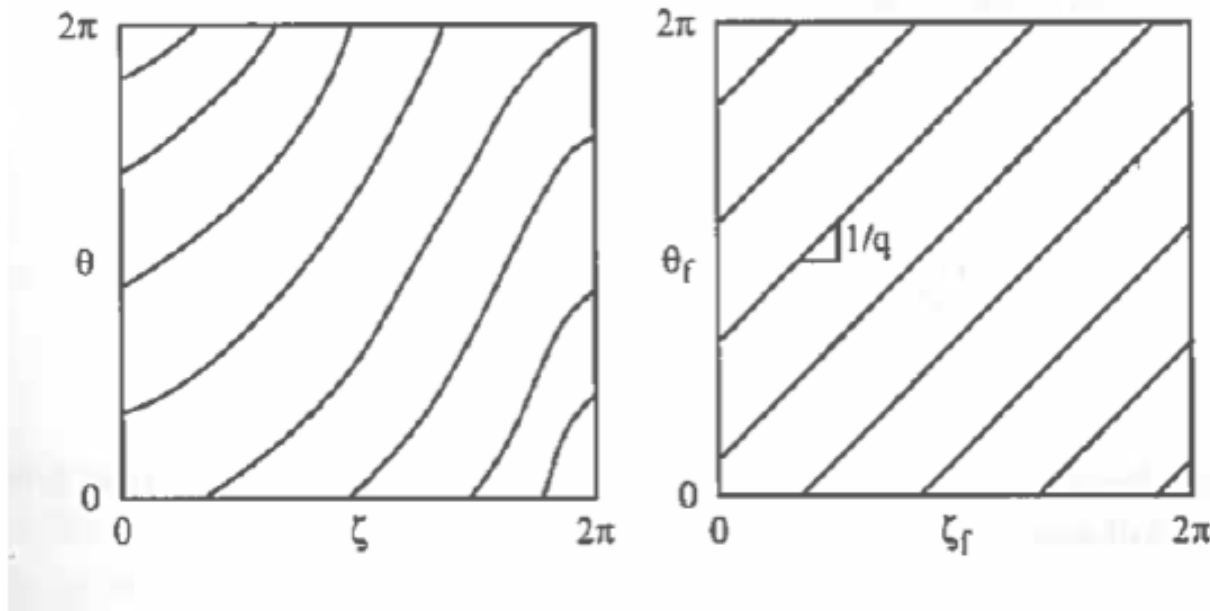
$$L = P_\theta \dot{\theta} + P_\zeta \dot{\zeta} + \frac{mc}{e} \mu \dot{\xi} - H(P_\zeta, P_\theta, \theta, \mu)$$

$$P_\theta = \frac{eA_\theta}{c} + mv_\parallel \frac{B_\theta}{B} \quad P_\zeta = \frac{eA_\zeta}{c} + mv_\parallel \frac{B_\zeta}{B}$$

- We need to find global flux coordinate system that can be used in realistic tokamak simulation.

# Revisiting straight field line coordinates

- Straight field line coordinates are magnetic flux coordinates, in which the poloidal or toroidal magnetic flux ( $\psi_p$  or  $\psi$ ) is used as the radial coordinate.
- Poloidal ( $\theta$ ) and toroidal angles ( $\zeta$ ) are defined so that the field line is straight in the  $(\theta, \zeta)$  plane.



- The corresponding vector potential is  $A = \psi \nabla \theta - \psi_p \nabla \zeta$ , the safety factor is  $q = d\psi_p/d\psi$  and magnetic field is  $B = \nabla \psi \times \nabla \theta + \nabla \zeta \times \nabla \psi_p$

# Existing flux coordinates

- Straight field line coordinates are not unique. Here are some flux coordinates that are commonly used:

Flux coordinate type	Characteristic
PEST	Toroidal angle is the geometric angle
BOOZER	Specify Jacobian to $1/B^2$
HAMADA	Specify Jacobian to unity
EQARC	Equal Arc length coordinate

- The common advantage of straight field line coordinates is that they facilitate the separation of plasma effects along and perpendicular to magnetic field lines for magnetized plasmas.
- We seek for “**canonical straight field line coordinates**”, to eliminate  $B_\psi$  while maintaining the property of straight field line coordinate.

# Coordinate transformation equation

We introduce a function  $v(\psi, \theta)$  and transform the toroidal and poloidal angles simultaneously ( $\theta_c = \theta + v(\psi, \theta)$ ;  $\zeta_c = \zeta + qv(\psi, \theta)$ ), so that the new coordinates has straight field line as the general flux coordinate.

Then the vector potential preserves:  $A = \psi \nabla \theta_c - \psi_p \nabla \zeta_c$ .

**Thus the only constraint to canonical field is**

$$\mathbf{B} \cdot \nabla \theta_c \times \nabla \zeta_c = 0$$

We then end up with a nonlinear equation for  $v$

$$\frac{\partial v}{\partial \psi} = C_1 \frac{\partial v}{\partial \theta} + C_2 v \frac{\partial v}{\partial \theta} + C_2 v + C_1 \quad (3)$$

with

$$-C_1 = \frac{G_{12} + qG_{31}}{G_{22} + 2qG_{23} + q^2G_{33}}, C_2 = -q' \frac{G_{23} + qG_{33}}{G_{22} + 2qG_{23} + q^2G_{33}}$$

-where  $G_{12}, G_{31}, G_{22}, G_{33}, G_{23}$  are the equilibrium matrices.

# Ordering in the transformation equation

We found there is an apparent ordering in Eq. (3), in PEST coordinates

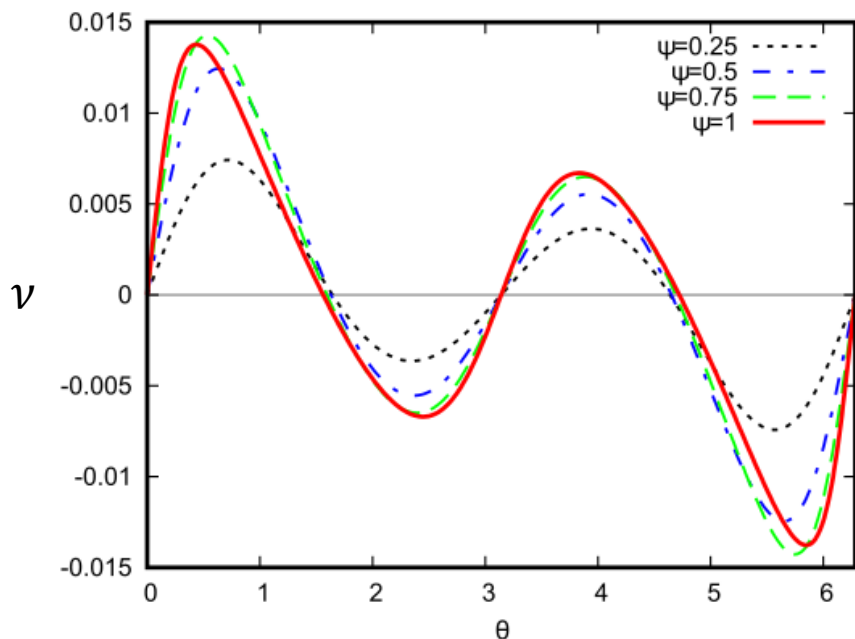
$$C_1 \sim \frac{|\nabla\phi|^2 (\nabla\psi \cdot \nabla\theta)}{q^2 |\nabla\psi \cdot \nabla\theta|^2} \sim \varepsilon^2, C_2 \sim 1$$

**The ordering indicates that for large aspect ratio tokamak, the modification to the poloidal angle is relatively small, which ensures a global solution to the equation.**

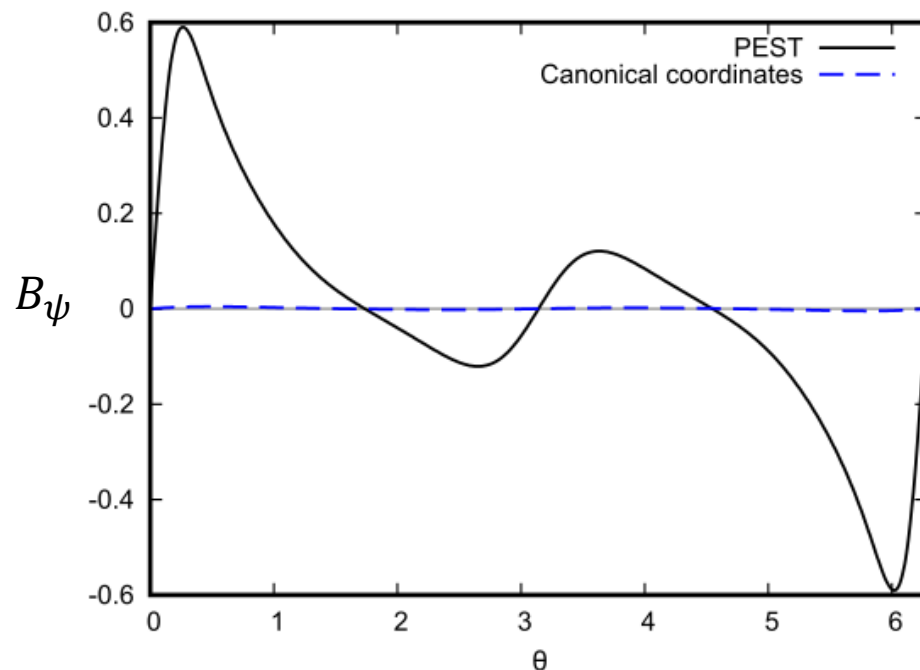
- Note that  $\nu$  has to satisfy the periodic boundary condition in  $\theta$ , we use Fourier transform and set  $\nu$  to zero at the magnetic axis to integrate equation (3) numerically.

# Implementation of the new coordinates

- With the ITER-like equilibrium, we start from PEST coordinates and compare the resulting canonical straight field line coordinates with PEST.



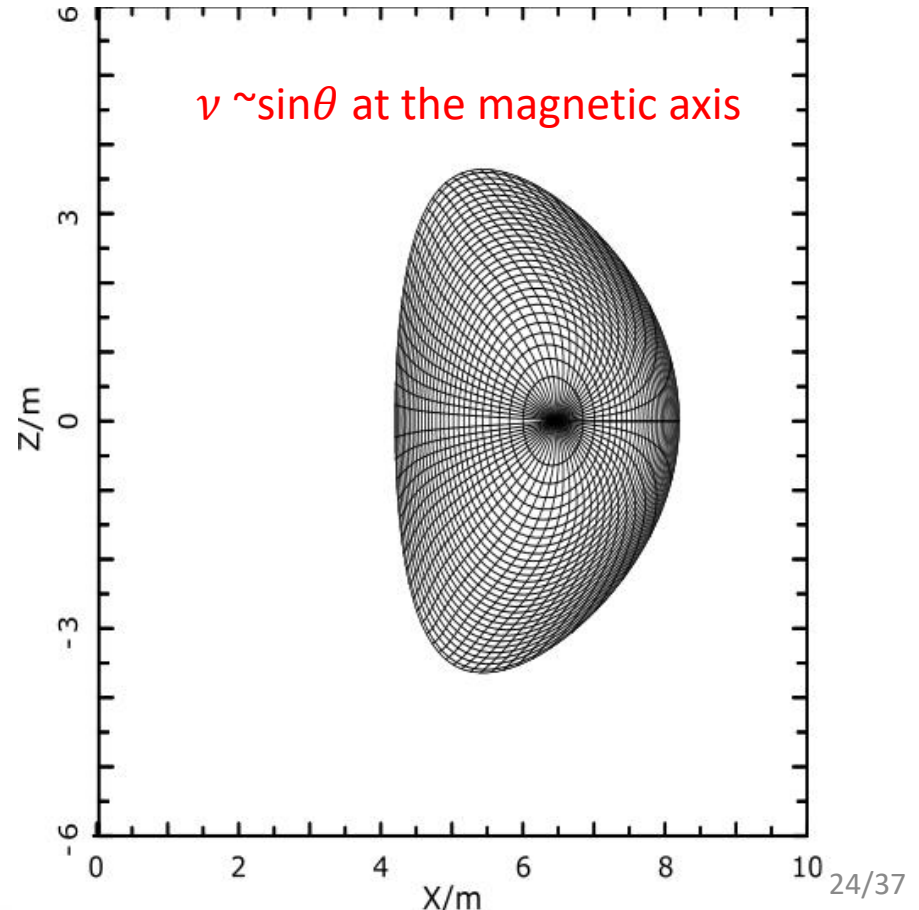
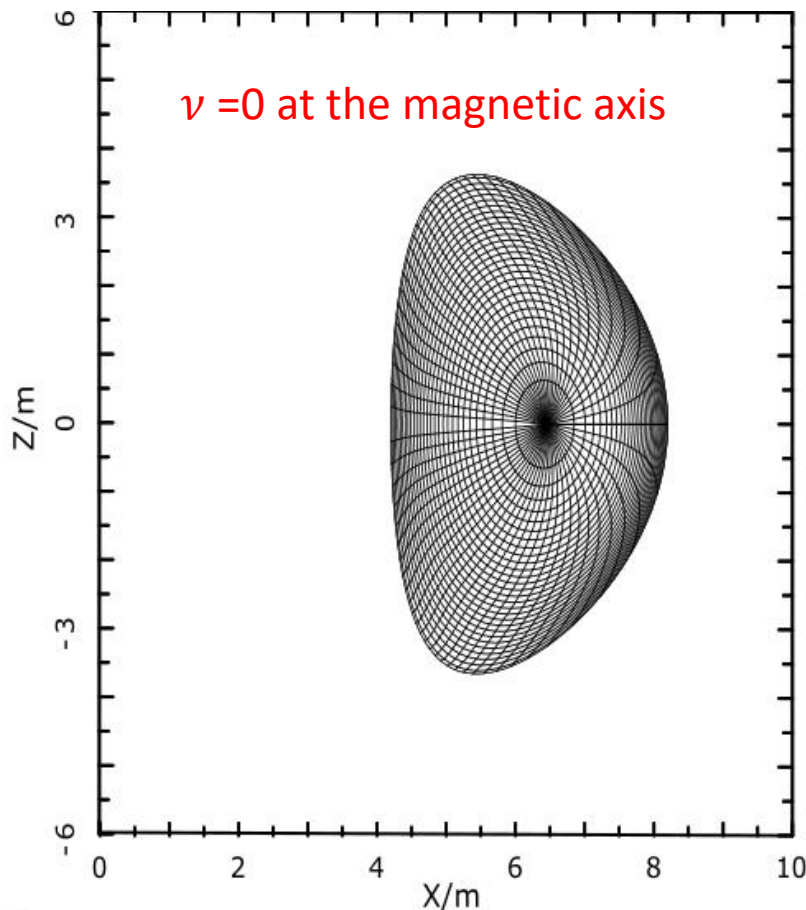
The difference in poloidal angle between PEST and new coordinates is very small.



$B_\psi$  vanishes in canonical straight field line coordinates.

# Boundary condition effects

- The grid mesh of canonical straight field line coordinates can change with boundary conditions



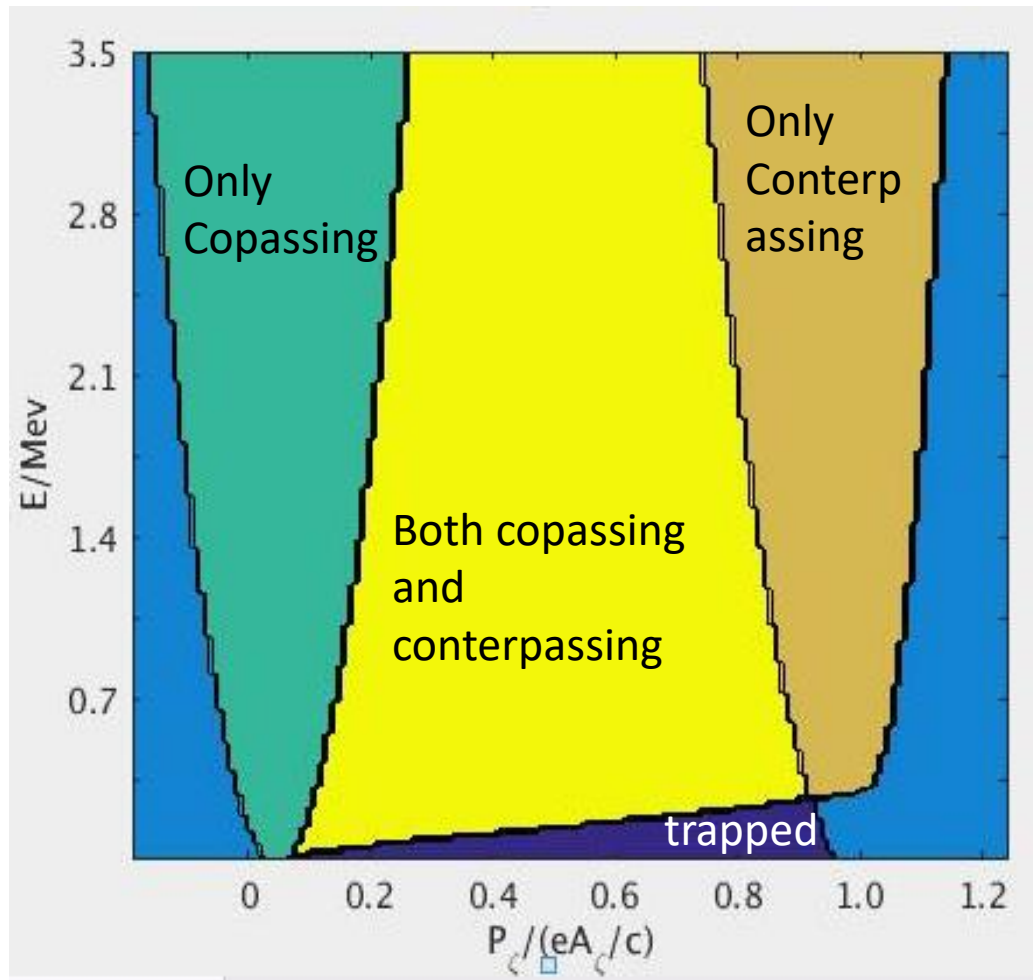


# Remarks about the canonical straight field line coordinates

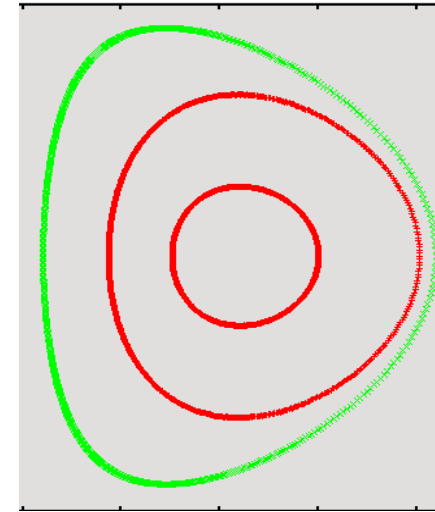
- The new magnetic flux coordinates are convenient for both particle simulation and MHD simulation.
- Correction to the poloidal and toroidal angles are small.
- The radial component of the magnetic field vanishes in the new coordinate, thus enabling a Hamiltonian description of the GC motion.
- There are multiple ways to perform the transformation.

M. Li et al., *Journal of Computational Physics*, **326** 324 (2016).

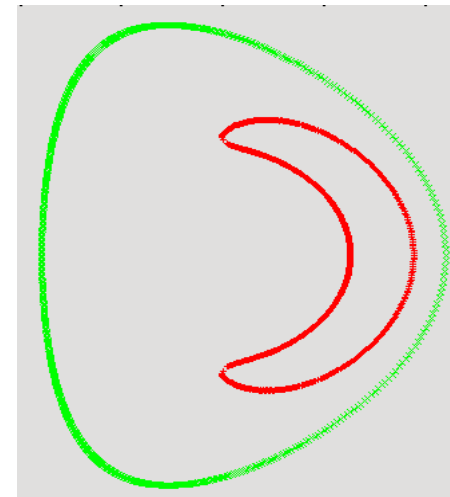
# Guiding center orbits in the ITER-like equilibrium



Different orbit types given fixed  $\mu$



Passing particle orbit



Banana particle orbit

# Outline

- **MHD stability analysis for Alfvénic Modes**
  1. AEGIS framework
  2. Continuum absorption near TAE gap
- **Energetic Particle dynamics**
  1. Canonical Straight field line coordinates
  2. Scheme for constructing Action-Angle variables

# Advantage of Action-Angle variables

With canonical straight field line coordinates, we are able to describe transport of resonant energetic particles in the Action-Angle variables associated with unperturbed guiding center orbit.

## Benefits:

- **The equilibrium orbit is separated from the perturbed motion.**
- **It is easier to identify resonant particles.**
- **Wave and particle interaction can be simplified to the 1D bump-on-tail problem for single resonance cases.**

# Action-Angle variables for unperturbed GC motion

- The unperturbed GC motion is fully integrable, we consider the generating function:

$$G = \zeta \widetilde{P}_\zeta + \xi \frac{mc}{e} \tilde{\mu} + \int_0^\theta P_\theta [\widetilde{H}; \widetilde{P}_\zeta; \tilde{\mu}; \theta] d\theta$$

which will give us the action-angle variables.

The Lagrangian is

$$L = \widetilde{P}_\zeta \dot{\zeta} + \widetilde{P}_\theta \dot{\theta} + \frac{mc}{e} \tilde{\mu} \dot{\xi} - H(\widetilde{P}_\zeta, \widetilde{P}_\theta, \tilde{\mu})$$

and the actions are constants of motion.

- We then numerically construct the coordinate transformation in particle phase space from  $(v_\parallel, \psi, \theta, \zeta)$  to  $(\widetilde{P}_\zeta, \widetilde{P}_\theta, \tilde{\zeta}, \tilde{\theta})$

# Hamiltonian with perturbed fields

- In the presence of a general perturbed field, we can modify the coordinate and momentum to retain the Hamiltonian form.

$$\theta = \theta_n + f(\psi, \theta, \zeta, t) \quad P_{\theta_n} = P_\theta + \Delta P_\theta(v_\parallel, \psi, \theta, \zeta, t)$$

$$\zeta = \zeta_n + g(\psi, \theta, \zeta, t) \quad P_{\zeta_n} = P_\zeta + \Delta P_\zeta(v_\parallel, \psi, \theta, \zeta, t)$$

where  $f$  and  $g$  are functions of the perturbed fields.

- The difference between new canonical momenta from the unperturbed ones is proportional to perturbed field  $E$ , which is relatively small compared to the change of resonant particle momentum by the waves ( $\sim \sqrt{E}$ ).
- We can then use the unperturbed momentum (and the unperturbed action-angle variables) to describe the perturbed Hamiltonian.

# Perturbed Hamiltonian in the Action-Angle variables

- The perturbed Hamiltonian is

$$H = H_0(\widetilde{P}_\zeta, \widetilde{P}_\theta, \widetilde{\mu}) + H_1(\widetilde{P}_\zeta, \widetilde{P}_\theta, \widetilde{\mu}, \widetilde{\zeta}, \widetilde{\theta}, t)$$

- Take into account the periodic boundary condition in terms of angles for the perturbation,

$$H = H_0(\widetilde{P}_\zeta, \widetilde{P}_\theta, \widetilde{\mu}) + \sum V_1(\widetilde{P}_\zeta, \widetilde{P}_\theta, \widetilde{\mu}, n, l) \exp(il\widetilde{\theta} + in\widetilde{\zeta} - i \int \omega(t) dt)$$

where

$$V_1(\widetilde{P}_\zeta, \widetilde{P}_\theta, \widetilde{\mu}, n, l) = \frac{1}{(2\pi)^2} \int_0^{2\pi} \int_0^{2\pi} H_1(\widetilde{P}_\zeta, \widetilde{P}_\theta, \widetilde{\mu}, \widetilde{\zeta}, \widetilde{\theta}, t) e^{-il\widetilde{\theta} - in\widetilde{\zeta}} d\widetilde{\zeta} d\widetilde{\theta}$$

The summation adds up the contribution for all resonances.

# Reducing to one dimensional

- In the case of single resonance without overlapping

$$H = H_0(\widetilde{P}_\zeta, \widetilde{P}_\theta, \tilde{\mu}) + V_1(\widetilde{P}_\zeta, \widetilde{P}_\theta, \tilde{\mu}, n, l) \exp(il\tilde{\theta} + in\tilde{\zeta} - i \int \omega(t) dt)$$

- We can transform the Hamiltonian to

$$H = H_0(p, J, \tilde{\mu}) + V_1(p, J, \tilde{\mu}, n, l) \exp(iq - i \int \omega(t) dt)$$

where

$$p = \frac{\widetilde{P}_\zeta}{l}, q = l\tilde{\theta} + n\tilde{\zeta}$$

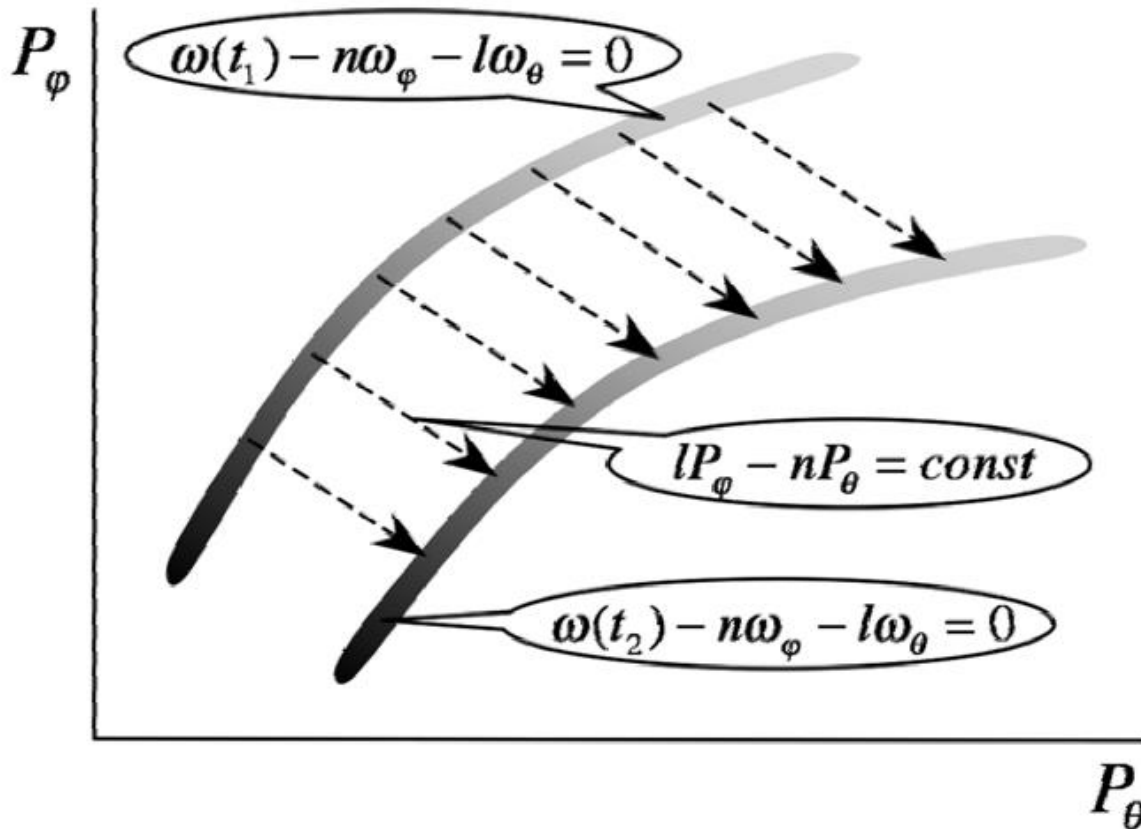
and  $J = l\widetilde{P}_\zeta - n\widetilde{P}_\theta$  is another conserved quantity as  $\mu$

- Similar to the process gyro-averaging, the Vlasov equation is reduced to 1D

$$\frac{\partial \delta f}{\partial t} + \left( n\omega_\zeta + \frac{\partial H_1}{\partial p} \right) \frac{\partial \delta f}{\partial q} - \frac{\partial H_1}{\partial q} \frac{\partial \delta f}{\partial p} = \frac{\partial H_1}{\partial q} \frac{\partial F_0}{\partial p}$$

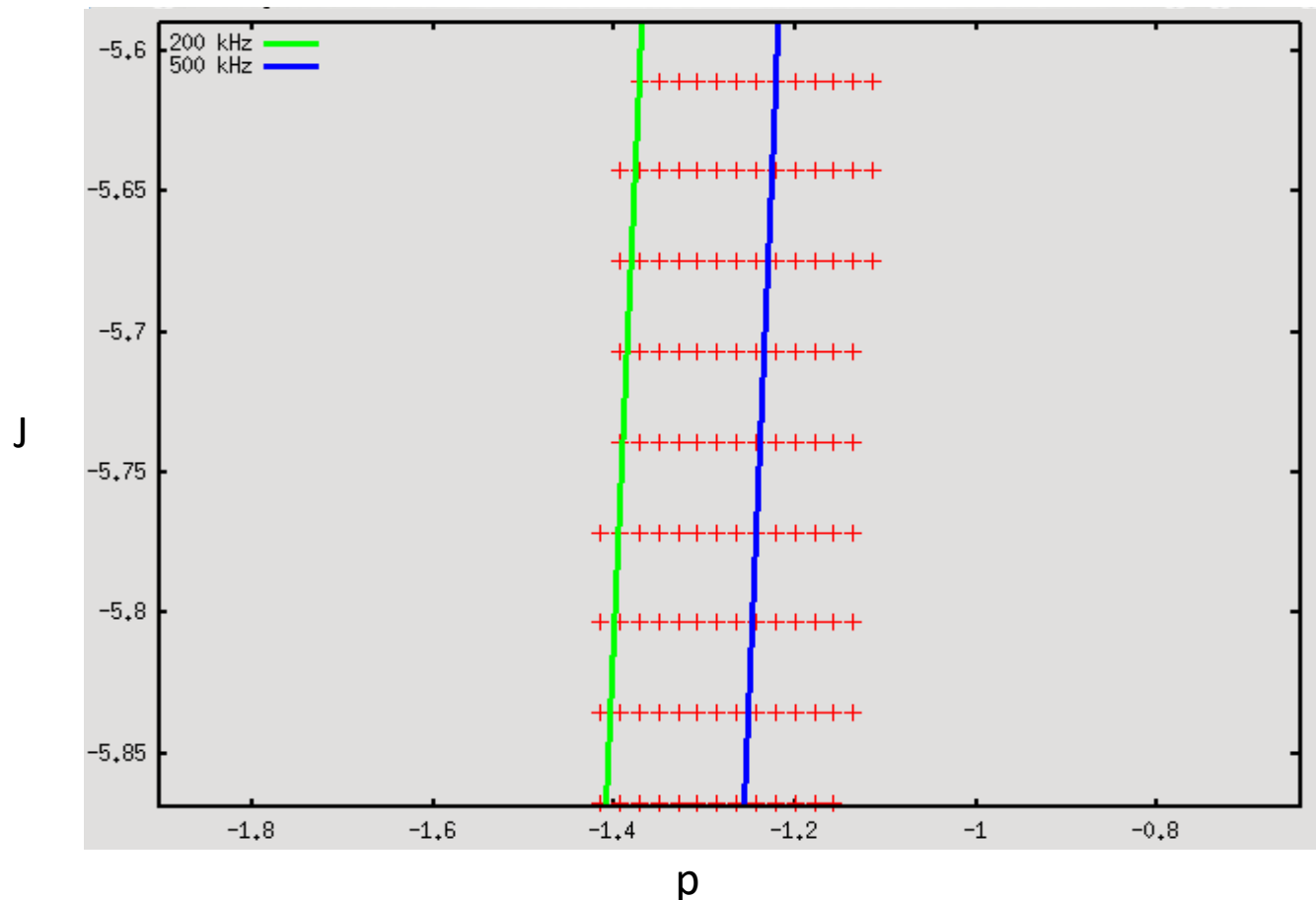


# Transport of resonant particles in Action-Angle coordinates



In nonlinear frequency sweeping events, a group of trapped particles slow down without losing coherency, resulting in considerable frequency shifts.\*

# Computation grid mesh for the single resonant case



We generate numerically mesh of  $(J, p)$  with resonant number  $n = 1, l = 1$  for the compassing particles, with resonant frequency labeled and the value of perturbed Hamiltonian stored on every grid point.

# Nonlinear wave-particle interaction closure-ongoing

- After calculation of the Vlasov equation in Action-Angle variables, the distribution function needs to be transformed and integrated in the AEGIS and complete the closure.
- The unfinished piece is to change the ideal MHD code AEGIS from eigenvalue to initial value code, to calculate the nonlinear wave and particle interaction.

# Summary

- Continuum absorption is evaluated on the basis of AEGIS, to resolve the different absorption features near TAE gap.
- “Canonical straight field line coordinates” are introduced, which provide a Hamiltonian description of particle guiding center motion while maintaining the conventional straight field line feature.
- Action-Angle coordinate system is constructed in the new magnetic flux coordinates, so that single resonance problem is simplified to one dimensional.
- Future work about nonlinear evolution of energetic-particle-driven mode is on the way.

**Questions?**